

Article

Thermal Properties of TiO₂NP/CNT/LDPE Hybrid Nanocomposite Films

Moustafa M. Zagho ^{1,2,*}, Mariam Al Ali AlMaadeed ^{1,2,*} and Khaliq Majeed ^{2,3} ¹ Materials Science and Technology Program, College of Arts and Sciences, Qatar University, Doha 2713, Qatar² Center for Advanced Materials, Qatar University, Doha 2713, Qatar; khaliqmajeed@gmail.com³ Department of Chemical Engineering, COMSATS University Islamabad, Lahore Campus, Lahore 54000, Pakistan

* Correspondence: mmsalah@qu.edu.qa (M.M.Z.); m.alali@qu.edu.qa (M.A.A.A.); Tel.: +974-4403-4384 (M.M.Z.); +974-4403-3990 (M.A.A.A.)

Received: 14 October 2018; Accepted: 12 November 2018; Published: 15 November 2018



Abstract: This work aims to investigate the effect of hybrid filler concentration on the thermal stability of low-density polyethylene (LDPE) matrices. LDPE-based composite films were synthesized by melt mixing, followed by compression molding, to study the influence of titanium oxide nanoparticles (TONPs) and/or multi-walled carbon nanotubes (CNTs) on the thermal properties of LDPE matrices. Fourier transform infrared (FTIR) spectroscopy confirmed the slight increase in the band intensities after TONP addition and a remarkable surge after the incorporation of CNTs. The value of crystallization temperature (T_c) was not modified after incorporating TONPs, while an enhancement was observed after adding the hybrid fillers. The melting temperature (T_m) was not changed after introducing the CNTs and CNT/TONP hybrid fillers. The percentage crystallinity (X_c %) was increased by 4% and 6%, after incorporating 1 wt % and 3 wt % CNTs, respectively. The TONP incorporation did not modify the X_c %. Moreover, thermal gravimetric analysis (TGA) thermograms confirmed the increased thermal stability after introducing CNTs and hybrid fillers compared to TONP incorporation.

Keywords: polymer composites; LDPE; TONPs; CNTs; morphological properties; thermal properties

1. Introduction

The materials manufactured from polyolefins, such as polyethylene (PE) and polypropylene (PP), have large commercial production due to their durability, light weight, low cost, and excellent mechanical properties [1]. Fabricating thermally stable polymers is highly needed in modern society [2]. Polymer nanocomposites are potential materials for different applications because of their unique properties [3–8]. Low-density polyethylene (LDPE) is a common polymer applied in different uses including industrial and space applications [9–13]. LDPE is widely used in the space craft industry because of its interesting characteristics, including chemical resistance, high flexibility, light weight, low cost of processing, and excellent tensile and thermal stability properties [14–16]. When titanium oxide nanoparticles (TONPs) are incorporated into the polymer, a system for biomedical applications is formed for antibacterial activity and odor inhibition [17,18]. Zapata et al. [19] reported the effect of TO and TONP dispersion on the dynamic, mechanical, thermal, and catalytic behaviors of PE and linear LDPE (LLDPE) composites. Ethylene homopolymer and ethylene-*co*-1-octadecene copolymers with 0.063 mol/L (LLDPE-1) and 0.38 mol/L (LLDPE-2) were prepared using a metallocene catalyst to prepare in situ TO-based composites. It was realized that the dispersion of TO in PE galleries was better than that in LLDPE-2 chains. The thermal stability of the polymers was improved significantly after TONP incorporation. The decomposition temperature of the prepared composites was raised

by 25 °C compared to the neat polymer. The mechanical results of TO/PE were different from that of TO/LLDPE-1 nanocomposites. Moreover, the tensile characteristics of TO/PE and TO/LLDPE-1 composites did not change compared to the neat polymer. The Young's modulus and yield stress of LLDPE-2 galleries were improved after incorporating 3 wt % and 5 wt % TONPs.

Carbon nanotubes (CNTs) represent a common promising reinforcing filler for polymers, as they can enhance the thermal and mechanical properties of the pristine polymers [20–22]. The topology and the final properties of polymer/CNT composites are controlled by the nature of chemical interactions between the polymer galleries and CNTs [23]. The impact of multi-walled CNT loadings on the thermal characteristics of polypropylene (PP) composites was investigated by Zhou et al. [24]. The results showed that the decomposition temperatures were shifted to higher values, and the maximum mass loss rate declined roughly with increasing CNT weight fraction. Furthermore, the residues increased linearly with higher CNT contents. A 10% increase in tensile stiffness and a slight rise in tensile strength were observed in a multi-walled CNT/polystyrene (MWCNT/PS) composite system [25]. Recent reports mentioned the limited uses of natural fiber/polymer composites because of their low impact behavior [26]. Of these, Puttegowda et al. discussed the potential aerospace uses of synthetic polymer composites [27]. In addition, the application of polyhedral oligomeric silsesquioxanes (POSSs) for producing composites was developed extensively in recent years because POSSs exhibit the property of being molecules when compared with the other most commonly applied fillers [28]. In addition, polyvinylidene fluoride (PVDF) matrices exhibited promising characteristics when reinforced with CNTs and other fillers [29–31]. Our team worked on different types of hybrid composites [32–34]. Based on the abovementioned significance of these two fillers, this work pursues a means of comparative analysis of LDPE nanocomposite films with different types of additives. The influence of TONPs, CNTs, and TONP/CNT combinations on the morphological and thermal properties of LDPE matrices is discussed in this paper. This work aims to realize the effect of hybrid filler content on the thermal behavior of LDPE matrices.

2. Materials and Methods

2.1. Materials

LDPE used in the composite films was procured from Qatar Petrochemical Company (QAPCO). Titanium (IV) oxide anatase nanopowder (TONPs) (particle size of 15 nm, 232033) and multi-walled carbon nanotubes (CNTs; outer diameter \times length: 6–9 nm \times 5 μ m; bulk density of 0.22 kg/m³; <95% carbon; 724769-25G) were obtained from Sigma-Aldrich (Saint Louis, MO, USA). All materials were used without any treatment.

2.2. Preparation of TONP/LDPE, CNT/LDPE, and TONP/CNT/LDPE Composite Films

LDPE-based composites were prepared using Brabender Plastograph EC batch mixer (Figure 1). The composites were blended with different contents of LDPE, TONPs, and/or CNTs to study the effect of filler content on the structural and thermal characteristics of LDPE matrices. The detailed composition of each sample and their designations are shown in Table 1. The mixing step was carried out at 180 °C and 50 rpm for a total duration of 10 min [35–37]. Then, the mixed composite lumps were pressed into sheets using a compression mounting press at 2 tons for 5 min at 180 °C. Finally, all prepared sheets were cooled to room temperature.

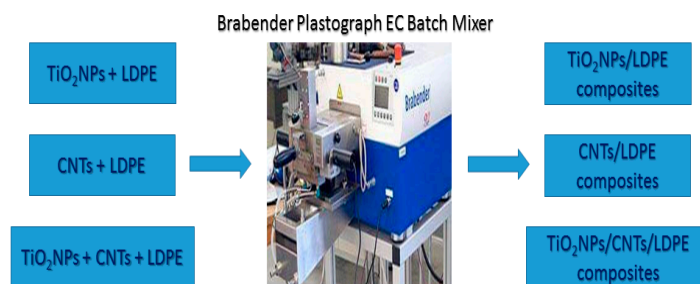


Figure 1. Illustrative diagram of mixing procedure.

Table 1. Designation and formulation of the synthesized low-density polyethylene (LDPE)-based composite films. TONP—titanium oxide nanoparticle; CNT—carbon nanotube.

Sample Designation	wt % TONPs	wt % CNTs	wt % LDPE
B1	0	0	100
B2	1	0	99
B3	2	0	98
B4	0	1	99
B5	0	3	97
B6	0	5	95
B7	2	1	97
B8	2	3	95
B9	2	5	93

2.3. Film Characterization

2.3.1. X-ray Diffraction (XRD)

The morphology of LDPE composites was investigated using XRD measurements. A MiniFlexII X-ray Diffractometer (Rigaku, Tokyo, Japan) was equipped at room temperature to perform XRD analysis of the neat LDPE and LDPE-based composite films. This technique was employed with a Cu-K α source ($\lambda = 1.5404 \text{ \AA}$). It was performed at 50 kV and 20 mA [38–40]. The results were achieved in a 2θ range from 2° to 80° , with a 0.1° step size.

2.3.2. Scanning Electron Microscopy (SEM)

A NOVA NANOSEM 450 (FEITM, Brno, Czech Republic) was used to investigate the composite structure (voltage of 500 V to 30 kV). All as-prepared films were firstly plasma-etched to study the dispersion of the fillers into LDPE matrices. The samples with a fractured surface were produced by breaking the composites in liquid N₂. All films were then coated by a thin film of gold in a sputtering chamber on the SEM holder.

2.3.3. Fourier Transform Infrared Spectroscopy (FTIR)

A Frontier FTIR spectrometer (Perkin Elmer, Shelton, CT, USA) was used to investigate the interfacial interactions between the LDPE galleries and the additives using FTIR spectra. This spectrometer worked in attenuated total reflectance (ATR) mode. The spectra of the films were measured in the range of 4000–450 cm⁻¹.

2.3.4. Differential Scanning Calorimetry (DSC)

Differential scanning calorimetry was performed to determine the melting temperature (T_m), crystallization temperature (T_c), and percentage crystallinity (X_c %) using a Jade DSC (PerkinElmer, Shelton, CT, USA). Initially, 5 mg of all films were heated from 30°C to 180°C , before being cooled to 30°C and heated again to 180°C . This procedure is a typical one that is used in the literature to conduct DSC experiments [41]. The first scan is to erase the thermal hysteresis of the sample, while the cooling

is to record the recrystallization, and the third step is to record the T_m value [41]. The heating and cooling rates were set at 10 °C/min. Nitrogen gas was purged during measurements. The enthalpy of the melting process value (ΔH_f) was determined in J/g from the measured T_m value. The X_c % was calculated as shown in Equation (1), where ΔH_o is the melting enthalpy of polyethylene of 100% crystallinity and is equal to 290 J/g [42].

$$X_c \% = \frac{(\Delta H_f/W\%)}{\Delta H_o} \times 100. \quad (1)$$

2.3.5. Thermal Gravimetric Analysis (TGA)

A Pyris 6 TGA (PerkinElmer, Shelton, CT, USA) was used to obtain TGA thermograms of weight loss as a function of temperature under nitrogen atmosphere for the neat LDPE and LDPE nanocomposites. Samples were heated from 30 °C to 600 °C with a heating rate of 10 °C/min.

3. Results and Discussion

3.1. Morphological and Dispersion Properties of LDPE-Based Nanocomposites

Figure 2 represents the XRD spectra of LDPE and selected composites. The LDPE phase has two characteristic sharp peaks centered at 21.41° and 23.60°, corresponding to (110) and (200) planes, respectively [43]. The appearance of another characteristic peak at 25.05° in the composites having 2 wt % TONPs (B3 and B7) corresponds to the TiO₂ anatase phase. Furthermore, CNTs exhibit a characteristic XRD peak centered at 23.4°, corresponding to the (002) plane [44]. This peak is not shown in the spectra of the composites having 1 wt % CNTs (B4 and B7). This disappearance confirms the good dispersion of CNTs within the LDPE network, and the same observation was reported by Yurdakul et al. [45].

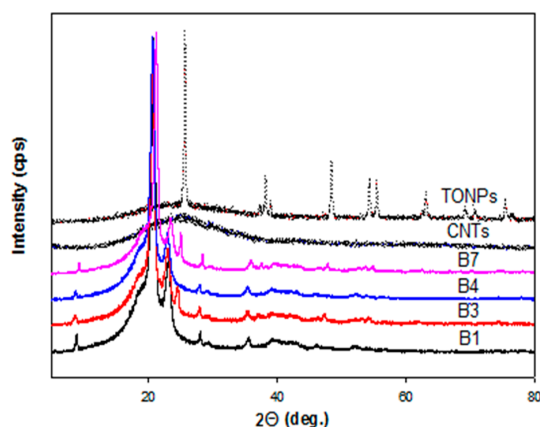


Figure 2. X-ray diffraction (XRD) patterns of TiO₂ powder, carbon nanotubes (CNTs), pristine low-density polyethylene (LDPE), and the representative composite films.

Surface topology of the additives and their dispersion into the polymer galleries was studied by Nano-SEM (N-SEM) and the representative images are demonstrated in Figure 3. This figure also compares the typical SEM micrographs of the composite films and the fractured surface. The images of the pure additives realized a spherical morphology of TONPs, while CNTs were tubular clusters and existed in entangled agglomerates. A micrograph of the sample containing 2 wt % TONPs (B3) confirmed that TONPs floated and dispersed well on the LDPE network, as shown in Figure 3. Flootation of the TONPs may be due to the poor compatibility between TONPs and LDPE chains. The dispersion of CNTs into the LDPE matrix was also poor, and entangled agglomerates of CNTs can be seen from the micrograph of the film containing 3 wt % CNTs (B5). The surface morphology of the composite films containing 2 wt % TONPs and 3 wt % CNTs (B8) illustrate that there are some pores

on the surface owing to plasma-etching. Furthermore, CNTs and TONPs were well dispersed and embedded throughout LDPE galleries. In such systems, the interactions were maximized; this can lead to remarkable changes in the thermal properties, as discussed in subsequent sections.

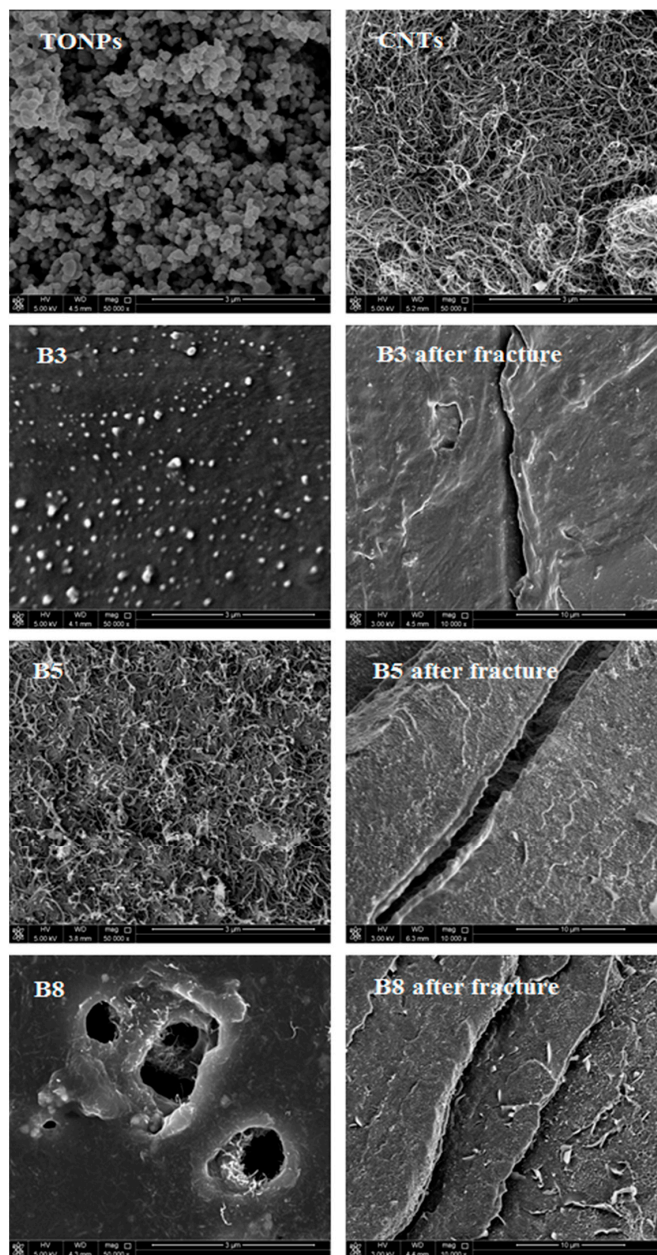


Figure 3. N-SEM images of titanium oxide nanoparticle (TONP) powder, CNTs, and the representative nanocomposites.

The fractured surface after breaking in liquid nitrogen and adding 2 wt % TONPs had fewer tracks compared to the 3 wt % CNT-filled films and was almost the same after simultaneous incorporation of 2 wt % TONPs and 3 wt % CNTs. This observation may be due to strong TONP–LDPE interfacial adhesion forces. The chemical interactions of fillers with the LDPE matrices were studied using FTIR spectroscopy, as shown in Figure 4. The pristine LDPE film demonstrates unique absorbance peaks at 2913, 2853, 1472, 1463, 729, and 719 cm^{-1} which correspond to CH_2 bending and stretching vibrations of the LDPE network [46]. The chemical composition of LDPE did not change after the addition of TONPs and/or CNTs. Furthermore, the band intensities increased slightly after adding 1 wt % and 2 wt % TONPs, while the incorporation of CNTs led to a significant rise in the band intensities due to

enhanced crystallinity (Figure 4), which is discussed in the subsequent sections [47]. The 719 cm^{-1} peak shifted to lower wave number if TONPs or/and CNTs were added. This shift may be attributed to the intermolecular interactions and forces between fillers and polymer chains [48,49]. The interfacial adhesion forces and intermolecular interactions between the fillers and LDPE matrices were confirmed upon correlating FTIR and SEM measurements.

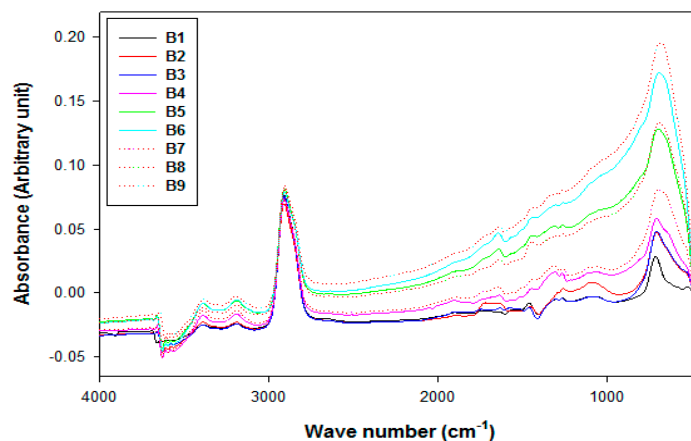


Figure 4. Fourier transform infrared (FTIR) spectra of LDPE and its composite films.

3.2. Thermal Behavior of LDPE-Based Nanocomposites

DSC thermograms were used to investigate the influence of TONP and/or CNT incorporation on T_m and T_c values of LDPE-based composites. Table 2 reports the DSC values of neat LDPE and LDPE-based composite films. From Table 2, it can be observed that the neat LDPE exhibited a T_c of $93\text{ }^\circ\text{C}$. The incorporated TONPs did not change the value of T_c significantly. In contrast, a rise in T_c value of $3\text{ }^\circ\text{C}$ was observed after incorporating 1 wt % CNTs. This increase can be ascribed to their role as a nucleating agent which offers nucleation positions on nanotube sidewalls for the LDPE matrix [50]. The T_c increased by $4\text{ }^\circ\text{C}$ for 3 wt % CNTs, and then reduced again to a T_c of $96\text{ }^\circ\text{C}$ for 5 wt % CNTs. Adding the hybrid additives increased the T_c and the ability of crystals to be formed at higher temperatures. The hybrid additive encouraged the growth and formation of crystallites in the polymer, as reported elsewhere [51,52]. The T_m after adding 1 wt % and 2 wt % TONPs increased by about $1\text{ }^\circ\text{C}$. It was not changed or modified after adding the CNTs. The same constant T_m was noticed for the hybrid additives. The X_c % calculated from DSC curves of the LDPE network increased after adding 1 wt % and 3 wt % CNTs by 4% and 6%, respectively. For the addition of 5 wt %, X_c % increased by 4%. The TONP addition did not change the X_c % much. The hybrid additives in B7 had a high X_c % value of 34%. The hybrid additives increased the packing of chains, and encouraged crystallinity.

Table 2. T_m , T_c , ΔH_m , and X_c % of the pristine LDPE and its composite films.

Sample Designation	T_m ($^\circ\text{C}$)	T_c ($^\circ\text{C}$)	ΔH_f (J/g)	X_c %
B1	108	93	87	30
B2	110	94	88	30
B3	110	94	90	32
B4	108	96	99	34
B5	109	97	102	36
B6	109	96	95	34
B7	109	96	94	34
B8	108	96	81	30
B9	108	96	82	30

TGA thermograms of neat LDPE and LDPE composites are shown in Figure 5. The pristine LDPE had single-stage degradation with 80% weight loss at 458 °C due to the C–C bond cleavage without leaving any residue [53–56]. In general, major weight losses were noted in the range of 400–550 °C, which corresponds to polymer degradation. Evidently, the thermal stability of TONP/LDPE systems was reduced compared to the pristine LDPE film. The TGA results of CNT/LDPE composites were quite in contrast to the corresponding ones reported earlier by Yang et al. [57]. The presence of hybrid additives increased the thermal stability of the composites, and this behavior was ascribed to the better dispersion of the fillers in the matrix [34,58]. This influence may be ascribed to the incorporated CNTs effectively preventing the diffusion of volatile decomposition products and the creation of stable free radicals [59,60]. After 550 °C, all TGA thermograms became flat, and mainly the residue remained. The TGA curves, highlighted in Figure 5, clearly reveal that the initial decomposition temperature (T_i) values attained for all CNTs and hybrid composites were higher than that of LDPE, thus emphasizing that the dispersion of CNTs in the polymer network does enhance the thermal stability of these composites. In contrast, the T_i values of TONP/LDPE systems were lower than that of LDPE, suggesting that the incorporation of TONPs does not offer thermal stability to these systems.

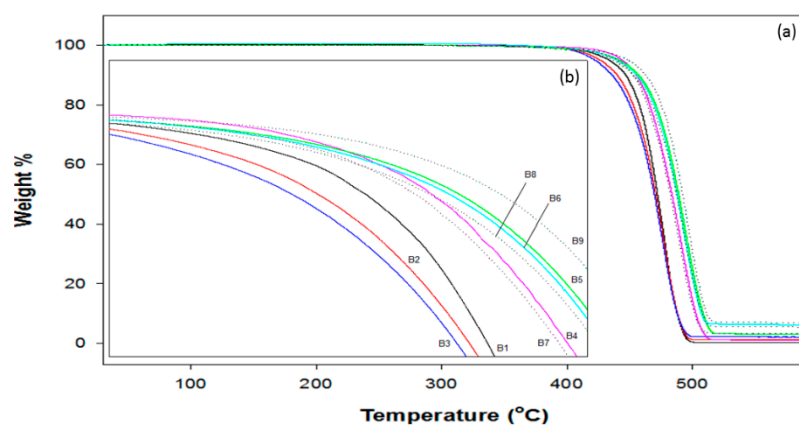


Figure 5. (a) Thermal gravimetric analysis (TGA) curves of pristine LDPE and its composite films. (b) Expanded degradation curves.

It can be revealed that the intermolecular interactions and interfacial adhesion forces between TONPs and/or CNTs with LDPE matrices were confirmed from the XRD, SEM, FTIR, DSC, and TGA experiments discussed in this work, and how the fillers' interactions enhanced the thermal properties of LDPE matrices by creating stable free radicals and preventing the diffusion of volatile decomposition products.

4. Conclusions

A successful method for enhancing the morphological and thermal characteristics of LDPE matrices was achieved by adding different contents of TONPs, CNTs, and TONPs/CNTs. The nanocomposites were processed by melt mixing followed by compression molding to prepare thin films. The added TONPs did not modify the value of T_c . On the other hand, an increase in T_c value of 3 °C was noticed after adding 1 wt % CNTs. Introducing the hybrid fillers enhanced the T_c and the ability of crystals to be produced at higher temperatures. The T_m after adding 1 wt % and 2 wt % TONPs increased by 1 °C. It was not modified after incorporating the CNTs and CNT/TONP hybrid fillers. The X_c % was improved after adding 1 wt % and 3 wt % CNTs by 4% and 6%, respectively. The TONP incorporation did not modify the X_c %. Furthermore, TGA curves showed the improved thermal stability after adding CNTs and hybrid fillers as compared to TONP addition. It can be summarized that the intermolecular interactions between TONPs and/or CNTs with LDPE matrices were confirmed from the different experiments addressed in this work, and how CNTs' interactions improved the thermal stability of LDPE matrices by preventing the diffusion of volatile decomposition products and creating stable free radicals.

Author Contributions: M.M.Z., M.A.A.A., and K.M. conceived and designed the experiments; M.M.Z. wrote the manuscript; M.A.A.A. supervised the writing and reviewed the manuscript.

Acknowledgments: This work was made possible by NPRP grant # (NPRP5-039-2-014) from the Qatar National Research Fund (a member of Qatar Foundation). The findings herein reflect the work, and are solely the responsibility of the authors. The publication of this article was funded by the Qatar National Library.

Conflicts of Interest: All authors of this article declare no conflict of interest.

References

1. Chum, P.S.; Swogger, K.W. Olefin polymer technologies—History and recent progress at The Dow Chemical Company. *Prog. Polym. Sci.* **2008**, *33*, 797–819. [[CrossRef](#)]
2. Blanco, I.; Abate, L.; Antonelli, M.L. The regression of isothermal thermogravimetric data to evaluate degradation Ea values of polymers: A comparison with literature methods and an evaluation of lifetime prediction reliability. *Polym. Degrad. Stab.* **2011**, *96*, 1947–1954. [[CrossRef](#)]
3. Zagho, M.M.; Hussein, E.A.; Elzatahry, A.A. Recent overviews in functional polymer composites for biomedical applications. *Polymers* **2018**, *10*, 739. [[CrossRef](#)]
4. Zagho, M.M.; Elzatahry, A. Recent Trends in Electrospinning of Polymer Nanofibers and their Applications as Templates for Metal Oxide Nanofibers Preparation. In *Electrospinning—Material, Techniques, and Biomedical Applications*; InTech: London, UK, 2016; pp. 3–24.
5. Khan, M.I.; Zagho, M.M.; Shakoor, R.A. A Brief Overview of Shape Memory Effect in Thermoplastic Polymers, Smart Polymer Nanocomposites. In *Smart Polymer Nanocomposites, Springer Series on Polymer and Composite Materials*; Springer International Publishing AG: New York, NY, USA, 2017; pp. 281–301.
6. Hussein, E.A.; Zagho, M.M.; Nasrallah, G.K.; Elzatahry, A.A. Recent advances in functional nanostructures as cancer photothermal therapy. *Int. J. Nanomed.* **2018**, *13*, 2897–2906. [[CrossRef](#)] [[PubMed](#)]
7. Dawoud, H.D.; Altahtamouni, T.M.; Zagho, M.M.; Bensalah, N. A brief overview of flexible CNT/PANI super capacitors. *Mater. Sci. Nanotechnol.* **2017**, *1*, 23–36.
8. Al-Enizi, A.M.; Zagho, M.M.; Elzatahry, A.A. Polymer-based electrospun nanofibers for biomedical applications. *Nanomaterials* **2018**, *8*, 259. [[CrossRef](#)] [[PubMed](#)]
9. AlMaadeed, M.A.; Nógellová, Z.; Mičušík, M.; Novák, I.; Krupa, I. Mechanical, sorption and adhesive properties of composites based on low density polyethylene filled with date palm wood powder. *Mater. Des.* **2014**, *53*, 29–37. [[CrossRef](#)]
10. Al-Ma'adeed, M.; Ozerkan, G.; Kahraman, R.; Rajendran, S.; Hodzic, A. Life cycle assessment of particulate recycled low density polyethylene and recycled polypropylene reinforced with talc and fiberglass. *Key Eng. Mater.* **2011**, *471–472*, 999–1004. [[CrossRef](#)]
11. Noorunnisa Khanam, P.; Al-Maadeed, M.A.; Mrlik, M. Improved flexible, controlled dielectric constant material from recycled LDPE polymer composites. *J. Mater. Sci. Mater. Electron.* **2016**, *27*, 8848–8855. [[CrossRef](#)]
12. Noorunnisa Khanam, P.; AlMaadeed, M.A.; Ouederni, M.; Harkin-Jones, E.; Mayoral, B.; Hamilton, A.; Sun, D. Melt processing and properties of linear low density polyethylene-graphene nanoplatelet composites. *Vacuum* **2016**, *130*, 63–71. [[CrossRef](#)]
13. Sobolciak, P.; Karkri, M.; Al-Maadeed, M.A.; Krupa, I. Thermal characterization of phase change materials based on linear low-density polyethylene, paraffin wax and expanded graphite. *Renew. Energy* **2016**, *88*, 372–382. [[CrossRef](#)]
14. Murray, K.A.; Kennedy, J.E.; McEvoy, B.; Vrain, O.; Ryan, D.; Cowman, R.; Higginbotham, C.L. The effects of high energy electron beam irradiation in air on accelerated aging and on the structure property relationships of low density polyethylene. *Nucl. Instrum. Methods Phys. Res. Sect. B Beam Interact. Mater. At.* **2013**, *297*, 64–74. [[CrossRef](#)]
15. Willis, P.B.; Hsieh, C.-H. Space applications of polymeric materials. *Kobunshi* **2000**, *49*, 52–56. [[CrossRef](#)]
16. Guetersloh, S.; Zeitlin, C.; Heilbronn, L.; Miller, J.; Komiyama, T.; Fukumura, A.; Iwata, Y.; Murakami, T.; Bhattacharya, M. Polyethylene as a radiation shielding standard in simulated cosmic-ray environments. *Nucl. Instrum. Methods Phys. Res. Sect. B Beam Interact. Mater. At.* **2006**, *252*, 319–332. [[CrossRef](#)]
17. Ward-Close, C.M.; Godfrey, A.B.; Thompson, S.R. Titanium made the EDO way should see prices drop. *Met. Powder Rep.* **2005**, *60*, 20–25. [[CrossRef](#)]

18. Tong, Y.; Li, Y.; Xie, F.; Ding, M. Preparation and characteristics of polyimide-TiO₂ nanocomposite film. *Polym. Int.* **2000**, *49*, 1543–1547. [[CrossRef](#)]
19. Zapata, P.A.; Palza, H.; Cruz, L.S.; Lieberwirth, I.; Catalina, F.; Corrales, T.; Rabagliati, F.M. Polyethylene and poly(ethylene-co-1-octadecene) composites with TiO₂ based nanoparticles by metallocenic “in situ” polymerization. *Polymer* **2013**, *54*, 2690–2698. [[CrossRef](#)]
20. Thostenson, E.T.; Li, C.; Chou, T.W. Nanocomposites in context. *Compos. Sci. Technol.* **2005**, *65*, 491–516. [[CrossRef](#)]
21. Moniruzzaman, M.; Winey, K.I. Polymer nanocomposites containing carbon nanotubes. *Macromolecules* **2006**, *39*, 5194–5205. [[CrossRef](#)]
22. Coleman, J.N.; Khan, U.; Blau, W.J.; Gun'ko, Y.K. Small but strong: A review of the mechanical properties of carbon nanotube-polymer composites. *Carbon* **2006**, *44*, 1624–1652. [[CrossRef](#)]
23. Mylvaganam, K.; Zhang, L.C. Chemical bonding in polyethylene-nanotube composites: A quantum mechanics prediction. *J. Phys. Chem. B* **2004**, *108*, 5217–5220. [[CrossRef](#)]
24. Zhou, T.Y.; Tsui, G.C.P.; Liang, J.Z.; Zou, S.Y.; Tang, C.Y.; Mišković-Stanković, V. Thermal properties and thermal stability of PP/MWCNT composites. *Compos. Part B Eng.* **2016**, *90*, 107–114. [[CrossRef](#)]
25. Wong, M.; Paramsothy, M.; Xu, X.J.; Ren, Y.; Li, S.; Liao, K. Physical interactions at carbon nanotube-polymer interface. *Polymer* **2003**, *44*, 7757–7764. [[CrossRef](#)]
26. Safri, S.N.A.; Sultan, M.T.H.; Jawaid, M.; Jayakrishna, K. Impact behaviour of hybrid composites for structural applications: A review. *Compos. Part B Eng.* **2018**, *133*, 112–121. [[CrossRef](#)]
27. Puttegowda, M.; Rangappa, S.M.; Jawaid, M.; Shivanna, P.; Basavegowda, Y.; Saba, N. Potential of natural/synthetic hybrid composites for aerospace applications. *Sustain. Compos. Aerosp. Appl.* **2018**, *315–351*. [[CrossRef](#)]
28. Blanco, I. The rediscovery of POSS: A molecule rather than a filler. *Polymers* **2018**, *10*, 904. [[CrossRef](#)]
29. Chamakh, M.M.; Ponnamma, D.; Al-Maadeed, M.A.A. Vapor sensing performances of PVDF nanocomposites containing titanium dioxide nanotubes decorated multi-walled carbon nanotubes. *J. Mater. Sci. Mater. Electron.* **2018**, *29*, 4402–4412. [[CrossRef](#)]
30. Parangusan, H.; Ponnamma, D.; Al-Maadeed, M.A.A. Stretchable electrospun PVDF-HFP/Co-ZnO nanofibers as piezoelectric nanogenerators. *Sci. Rep.* **2018**, *8*, 754. [[CrossRef](#)] [[PubMed](#)]
31. Ponnamma, D.; Erturk, A.; Parangusan, H.; Deshmukh, K.; Ahamed, M.B.; Al Ali Al-Maadeed, M. Stretchable quaternary phasic PVDF-HFP nanocomposite films containing graphene-titania-SrTiO₃ for mechanical energy harvesting. *Emergent Mater.* **2018**, *1*, 55–65. [[CrossRef](#)]
32. Al-Maadeed, M.A.; Shabana, Y.M.; Khanam, P.N. Processing, characterization and modeling of recycled polypropylene/glass fibre/wood flour composites. *Mater. Des.* **2014**, *58*, 374–380. [[CrossRef](#)]
33. AlMaadeed, M.A.; Kahraman, R.; Noorunnisa Khanam, P.; Madi, N. Date palm wood flour/glass fibre reinforced hybrid composites of recycled polypropylene: Mechanical and thermal properties. *Mater. Des.* **2012**, *42*, 289–294. [[CrossRef](#)]
34. Deshmukh, K.; Ahamed, M.B.; Deshmukh, R.R.; Pasha, S.K.K.; Sadasivuni, K.K.; Ponnamma, D.; AlMaadeed, M.A.A. Striking multiple synergies in novel three-phase fluoropolymer nanocomposites by combining titanium dioxide and graphene oxide as hybrid fillers. *J. Mater. Sci. Mater. Electron.* **2017**, *28*, 559–575. [[CrossRef](#)]
35. Kuplennik, N.; Tchoudakov, R.; Zelas, Z.B.-B.; Sadvski, A.; Fishman, A.; Narkis, M. Antimicrobial packaging based on linear low-density polyethylene compounded with potassium sorbate. *LWT Food Sci. Technol.* **2015**, *62*, 278–286. [[CrossRef](#)]
36. Majeed, K.; AlMaadeed, M.A.A.; Zagho, M.M. Comparison of the effect of carbon, halloysite and titania nanotubes on the mechanical and thermal properties of LDPE based nanocomposite films. *Chin. J. Chem. Eng.* **2018**, *26*, 428–435. [[CrossRef](#)]
37. Zagho, M.M.; AlMaadeed, M.A.A.; Majeed, K. Role of TiO₂ and Carbon Nanotubes on Polyethylene, and Effect of Accelerated Weathering on Photo Oxidation and Mechanical Properties. *J. Vinyl Addit. Technol.* **2018**. [[CrossRef](#)]
38. Kabalan, L.; Zagho, M.M.; Al-Marri, M.J.; Khader, M.M. Experimental and theoretical studies on the mechanical and structural changes imposed by the variation of clay loading on poly(vinyl alcohol)/cloisite[®] 93A nanocomposites. *J. Vinyl Addit. Technol.* **2018**. [[CrossRef](#)]

39. Zagho, M.M.; Khader, M.M. The Impact of Clay Loading on the Relative Intercalation of Poly (Vinyl Alcohol)—Clay Composites. *J. Mater. Sci. Chem. Eng.* **2016**, *4*, 20–31. [[CrossRef](#)]
40. Al-Marri, M.J.; Masoud, M.S.; Nassar, A.M.G.; Zagho, M.M.; Khader, M.M. Synthesis and characterization of poly(vinyl alcohol): Cloisite[®] 20A nanocomposites. *J. Vinyl Addit. Technol.* **2017**, *23*, 181–187. [[CrossRef](#)]
41. Urukawa, T.F.; Ato, H.S.; Ita, Y.K.; Atsukawa, K.M.; Amaguchi, H.Y.; Chiai, S.O.; Iesler, H.W.S.; Zaki, Y.O. Molecular Structure, Crystallinity and Morphology of Polyethylene/Polypropylene Blends Studied by Raman Mapping, Scanning Electron Microscopy, Wide Angle X-ray Diffraction, and Differential Scanning Calorimetry. *Polym. J.* **2006**, *38*, 1127–1136. [[CrossRef](#)]
42. Wunderlich, B. The Basis of Thermal Analysis. In *Thermal Characterization of Polymeric Materials*; Academic Press: New York, NY, USA, 1997; pp. 387–389.
43. Madani, M. Structure, optical and thermal decomposition characters of LDPE graft copolymers synthesized by gamma irradiation. *Curr. Appl. Phys.* **2011**, *11*, 70–76. [[CrossRef](#)]
44. Klanwan, J.; Akrapattangkul, N.; Pavarajarn, V.; Seto, T.; Otani, Y.; Charinpanitkul, T. Single-step synthesis of MWCNT/ZnO nanocomposite using co-chemical vapor deposition method. *Mater. Lett.* **2010**, *64*, 80–82. [[CrossRef](#)]
45. Yurdakul, H.; Durukan, O.; Seyhan, A.T.; Celebi, H.; Oksuzoglu, M.; Turan, S. Microstructural characterization of corn starch-based porous thermoplastic composites filled with multiwalled carbon nanotubes. *J. Appl. Polym. Sci.* **2013**, *127*, 812–820. [[CrossRef](#)]
46. Liu, G.; Liao, S.; Zhu, D.; Cui, J.; Zhou, W. Solid-phase photocatalytic degradation of polyethylene film with manganese oxide OMS-2. *Solid State Sci.* **2011**, *13*, 88–94. [[CrossRef](#)]
47. Navarro-Pardo, F.; Martínez-Barrera, G.; Martínez-Hernández, A.L.; Castaño, V.M.; Rivera-Armenta, J.L.; Medellín-Rodríguez, F.; Velasco-Santos, C. Effects on the thermo-mechanical and crystallinity properties of nylon 6,6 electrospun fibres reinforced with one dimensional (1D) and two dimensional (2D) carbon. *Materials* **2013**, *6*, 3494–3513. [[CrossRef](#)] [[PubMed](#)]
48. Konyushenko, E.N.; Stejskal, J.; Trchová, M.; Hradil, J.; Kovářová, J.; Prokeš, J.; Cieslar, M.; Hwang, J.Y.; Chen, K.H.; Sapurina, I. Multi-wall carbon nanotubes coated with polyaniline. *Polymer* **2006**, *47*, 5715–5723. [[CrossRef](#)]
49. Yuca, N.; Karatepe, N. Thermal and electrical properties of carbon nanotube based materials. *ACTA Phys. Pol. A* **2013**, *123*, 352–354. [[CrossRef](#)]
50. Mahmood, N.; Islam, M.; Hameed, A.; Saeed, S. Polyamide 6/ multiwalled carbon nanotubes nanocomposites with modified morphology and thermal properties. *Polymers* **2013**, *5*, 1380–1391. [[CrossRef](#)]
51. Al-Saygh, A.; Ponnamma, D.; AlMaadeed, M.; Vijayan, P.P.; Karim, A.; Hassan, M. Flexible pressure sensor based on PVDF nanocomposites containing reduced graphene oxide-titania hybrid nanolayers. *Polymers* **2017**, *9*, 33. [[CrossRef](#)]
52. Cicala, G.; Blanco, I.; Latteri, A.; Ognibene, G.; Bottino, F.A.; Elena, M. PES/POSS soluble veils as advanced modifiers for multifunctional fiber reinforced composites. *Polymers* **2017**, *9*, 281. [[CrossRef](#)]
53. Contat-Rodrigo, L.; Ribes-Greus, A.; Imrie, C.T. Thermal analysis of high-density polyethylene and low-density polyethylene with enhanced biodegradability. *J. Appl. Polym. Sci.* **2002**, *86*, 764–772. [[CrossRef](#)]
54. Xiang, H.; Sun, C.; Jiang, D.; Zhang, Q.; Dong, C.; Liu, L. Flame retardation and thermal degradation of intumescent flame-retarded polypropylene composites containing spiroporphoryldicyandiamide and ammonium polyphosphate. *J. Vinyl Addit. Technol.* **2010**, *16*, 161. [[CrossRef](#)]
55. Huang, N.H.; Chen, Z.J.; Wang, J.Q.; Wei, P. Synergistic effects of sepiolite on intumescent flame retardant polypropylene. *Express Polym. Lett.* **2010**, *4*, 743–752. [[CrossRef](#)]
56. Motaung, T.E.; Luyt, A.S.; Thomas, S. Morphology and properties of NR/EPDM rubber blends filled with small amounts of titania nanoparticles. *Polym. Compos.* **2011**, *32*, 1289–1296. [[CrossRef](#)]
57. Yang, J.; Li, X.; Liu, C.; Rui, E.; Wang, L. Effects of electron irradiation on LDPE/MWCNT composites. *Nucl. Instrum. Methods Phys. Res. Sect. B Beam Interact. Mater. At.* **2015**, *365*, 55–60. [[CrossRef](#)]
58. Blanco, I.; Bottino, F.A.; Cicala, G.; Latteri, A.; Recca, A. Synthesis and characterization of differently substituted phenyl hepta isobutyl-polyhedral oligomeric silsesquioxane/polystyrene nanocomposites. *Polym. Compos.* **2014**, *35*, 151–157. [[CrossRef](#)]

59. Motaung, T.E.; Luyt, A.S.; Bondioli, F.; Messori, M.; Saladino, M.L.; Spinella, A.; Nasillo, G.; Caponetti, E. PMMA-titania nanocomposites: Properties and thermal degradation behaviour. *Polym. Degrad. Stab.* **2012**, *97*, 1325–1333. [[CrossRef](#)]
60. Wang, H.; Xu, P.; Zhong, W.; Shen, L.; Du, Q. Transparent poly(methyl methacrylate)/silica/zirconia nanocomposites with excellent thermal stabilities. *Polym. Degrad. Stab.* **2005**, *87*, 319–327. [[CrossRef](#)]



© 2018 by the authors. Licensee MDPI, Basel, Switzerland. This article is an open access article distributed under the terms and conditions of the Creative Commons Attribution (CC BY) license (<http://creativecommons.org/licenses/by/4.0/>).